Journal of Solid State Chemistry 183 (2010) 1252–1257

Contents lists available at ScienceDirect

Journal of Solid State Chemistry

journal homepage: www.elsevier.com/locate/jssc

Improvement of the thermoelectric properties of $[Bi_{1.68}Ca_2O_{4-\delta}]^{RS}[CoO_2]_{1.69}$ cobaltite by chimie douce methods

Hervé Muguerra [a,*], Beatriz Rivas-Murias [a], Maria Traianidis [b], Catherine Henrist [a], Bénédicte Vertruyen [a], Rudi Cloots [a]

[a] Inorganic Materials Chemistry, Department of Chemistry, University of Liège, Allée de la Chimie 3 (Bât. B6), 4000 Liège, Belgium
[b] Belgian Ceramic Research Centre, Avenue Gouverneur Cornez 4, 7000 Mons, Belgium

ARTICLE INFO

Article history:
Received 7 December 2009
Received in revised form
5 March 2010
Accepted 22 March 2010
Available online 30 March 2010

Keywords:
Oxides
Layered cobaltite
Sol–gel technique
Spray-drying technique
Thermoelectric properties

ABSTRACT

$[Bi_{1.68}Ca_2O_{4-\delta}]^{RS}[CoO_2]_{1.69}$ has been obtained by different chimie douce methods and uniaxially or isostatically pressed. The influence of these parameters on the thermoelectric properties has been investigated. Contrary to the Seebeck coefficient, which remains unchanged, the electrical conductivity is greatly modified. In particular, spray-drying synthesis followed by uniaxial pressing results in an electrical conductivity two times larger than in the case of conventional solid state synthesis. Our results suggest that a narrow particle size distribution is beneficial to the thermoelectric properties of the layered compounds. The spray-drying technique seems to be promising to improve the electrical conductivity of layered materials. Moreover, this method presents other advantages (homogeneous samples and less energetic processing) which could be interesting to the future manufacturing of thermoelectric devices.

1. Introduction

Transition metal oxides have attracted much interest to solve the increasing demand in creation, storage and conversion of energy. An interesting solution is thermoelectricity, which converts directly thermal energy into electrical energy or vice versa. The thermoelectric (TE) devices provide an effective route to use the waste heat from automobiles or factories, or conversely to cool down electronic devices for example. The TE conversion efficiency is characterized by the figure of merit $ZT=S^2T/\rho\kappa$, where ρ, S and κ are the electrical resistivity, the Seebeck coefficient and the thermal conductivity, respectively. Consequently to obtain highly efficient TE devices, low ρ, high S and low κ must be associated simultaneously.

The layered cobalt oxides seem interesting candidates, due to their chemical stability and absence of hazardous elements such as Te, Se and Pb [1–5]. Their structure are described by two monoclinic subsystems alternating along the c axis [6–15]. A CoO_2 layer, formed by CoO_6 edge sharing octahedra, which is mainly responsible of the TE features and a rock salt (RS) block which is considered as an electron reservoir. The RS block can be formed by two, three or four layers. For example, the RS block of $[Ca_2CoO_{3-\delta}]^{RS}[CoO_2]_{1.62}$ is composed of three layers (CaO–CoO–CaO) [6] whereas $[Bi_{1.74}Sr_2O_{4-\delta}]^{RS}[CoO_2]_{1.82}$ includes four layers (SrO–BiO–BiO–SrO) [7]. The two monoclinic subsystems (i.e., CoO_2 layer and RS block) share the same a and c cell parameters but have different b parameters. This family of compounds is called "misfit" due to this incommensurability between the two subsystems. Their general chemical formula may be given by $[M_mA_2O_{2+m}]^{RS}[CoO_2]_q$, where M=Bi, Pb, Co…; A=Ca, Sr, Ba… and $q=b_1/b_2$ is the incommensurate ratio (b_1 is the b parameter of the RS block and b_2 of the CoO_2 layer).

Different methods have been used to improve the TE properties of these oxides. One approach consists in partial substitutions in the layers of the RS block. For $[Ca_2CoO_{3-\delta}]^{RS}[CoO_2]_{1.62}$, the ZT factor increases by substituting Bi [16], Na [17], or rare earth elements (e.g., Dy)[18] for Ca, and by substituting transition metals (Fe, Mn, Ni, Cu) for Co [19]. Due to the anisotropic properties of these oxides, another method for improving their TE properties is the fabrication of textured bulk ceramics. In fact, samples with well oriented grains exhibit an increase in electrical conductivity in comparison with randomly oriented samples. Different techniques have been reported, such as hot-forging techniques [20], spark plasma sintering [21], reactive templated grain growth [22] and magnetic alignment [23]. Moreover metallic particles, with lower electrical resistivity, can be added to cobaltite to improve their electrical conductivity [24]. For example, addition of Ag particles induces a small reduction of the Seebeck coefficient, whereas the electrical connection between the cobaltite grains is effectively improved. Finally, "chimie

* Corresponding author.
E-mail address: herve.muguerra@ulg.ac.be (H. Muguerra).

0022-4596/$ - see front matter © 2010 Elsevier Inc. All rights reserved.
doi:10.1016/j.jssc.2010.03.030

douce" techniques can be employed to obtain nanoparticles with good densification behavior and thereby to improve the TE properties. For example, it has been reported that $[Ca_2CoO_{3-\delta}]^{RS}[CoO_2]_{1.62}$ can be synthesized by polyacrylamide gel processing [25], polymerized complex [26], citrate sol–gel [27] and coprecipitation method [28].

The bismuth layered cobalt oxide $[Bi_{1.68}Ca_2O_{4-\delta}]^{RS}[CoO_2]_{1.69}$ (hereafter labeled BCCO) shows interesting thermoelectric properties: a large thermopower (typically $S_{300\,K}=140\,\mu V\,K^{-1}$), a low electrical resistivity (typically $\rho_{300\,K}=40\,m\Omega\,cm$) and a small thermal conductivity (typically $\kappa_{300\,K}=1\,W\,K^{-1}\,m^{-1}$) [29]. But its ZT value remains still lower than the $ZT=1$ criterion which is essential when considering the practical applications. Attempts to improve the ZT value have been tested hot-forging method [30] leading to textured materials appears promising due to the strong impact on electrical resistivity which decreases as the level of texturing increases.

In the present letter, we employ chimie douce techniques to try to improve the electrical conductivity of this material. By this approach, we hope to achieve comparable values than the ones obtained by hot forging-method, but with a lower energetic balance of synthesis process i.e., lower energy required to synthesize the sample. Indeed the packings have been realized only by cold uniaxial or isostatic pressing. In fact, the reduction of the energy required to synthesize the components of TE devices is an important aspect to their future commercialization.

We will focus on the influence of chimie douce processes and packing treatments on the microstructure, and then on the TE properties of BCCO.

2. Experimental procedure

Samples with nominal composition $[Bi_{1.68}Ca_2O_{4-\delta}]^{RS}[CoO_2]_{1.69}$ were prepared by different synthesis methods. In each case, the precursor powder was ground, uniaxially (100 MPa) or isostatically (225 MPa) pressed and sintered for 10 h at 1123 K in air.

2.1. Method 1, spray-drying technique

$CaCO_3$, $Co(CH_3COO)_2\cdot 4H_2O$ and $Bi(CH_3COO)_3$ were dissolved in aqueous acetic acid solution in the stoichiometric ratio: 2:1.69:1.68. The final cation concentration in the feedstock solution was ~0.10 mol/L and pH was ~5, suitable to avoid damaging the metallic parts of the spray-drying apparatus.

The solution was sprayed by a co-current Büchi Mini Spray Dryer B191, using a 0.7 mm nozzle. The inlet and outlet temperatures were 473 K and 418–423 K, respectively. The process used air as the carrier gas with a flow rate of 700 normal L/h. The liquid feed rate was 1.4 mL/min. After spray-drying, the precursor was precalcined at 873 K for 2 h.

2.2. Method 2, solid state reaction

$CaCO_3$, Co_3O_4 and Bi_2O_3 were thoroughly mixed and ground in an agate mortar in the molar ratio 2:0.563:0.84.

2.3. Method 3, sol–gel method

Stoichiometric mixtures of $CaCO_3$, $Co(NO_3)_2\cdot 6H_2O$ and Bi_2O_3 (2:1.69:0.84) were dissolved in an aqueous solution of nitric acid (total cation concentration ~0.30 mol/L). EDTA, used as chelating agent, was dissolved in an aqueous solution of NH_4OH. The metal cations solution was added dropwise to the EDTA solution. The molar ratio of metal cations to EDTA was 1:1.3. This final mixture was heated (while stirring) at 473 K to form a purple gel. The gel was burnt by a self-spread process at 573 K. The resulting precursor was calcined at 773 K for 5 h to remove residual organic compounds.

The X-ray powder diffraction measurements were carried out using a Siemens D5000 diffractometer equipped with Cu $K\alpha$ source at room temperature in air. The diffraction intensities were measured in the 2θ range from 10° to 70° at a step width of 0.020°. Environmental scanning electron microscope (FEG-ESEM, Philips XL30) with EDX analyzer was used to determine the cation ratio and the morphology of the particles. The density of the pellets was measured by Archimedes' method in 1-butanol. The average valence of cobalt, V(Co), were determined by iodometric titration. The sample (50 mg) is dissolved in 1 M HCl solution (100 mL) and subsequent reduce with I^- (KI, 2 g). I_2 was titrated with $Na_2S_2O_3$ solution (0.015 M) using starch as indicator. The experimental details were the same as described in Ref. [31]. Several parallel experiments confirmed reproducibility. The electrical conductivity and thermoelectric power were measured by a commercial RZ2001i device (Ozawa Science) from 300 to 1100 K in air.

3. Results and discussion

3.1. Structural and microstructural investigations

The X-ray powder diffraction (XRD) patterns of the BCCO samples are shown in Fig. 1. All patterns are similar and no impurities are detected. The cation ratios, evaluated by EDX analysis, are reported in Table 1, together with literature data for BCCO powder [29] and single crystal [32].

The cation ratios of the spray-drying and sol–gel samples agree with the single crystal composition ($[Bi_{1.68}Ca_2O_{4-\delta}]^{RS}[CoO_2]_{1.69}$ [32]) which is consistent with the cation ratios used for the synthesis (Table 1). In the case of the solid state samples, the composition is close to that previously reported [29]. Different reasons have been reported to explain the cobalt excess: the presence of small Co_3O_4 impurities (non-observable on the XRD pattern) or an inhomogeneous distribution of the stacking of the layers in the RS block ($[Bi_{1.7}Ca_2Co_{0.3}O_{4-\delta}]^{RS}[CoO_2]_{1.69}$) [29]. In

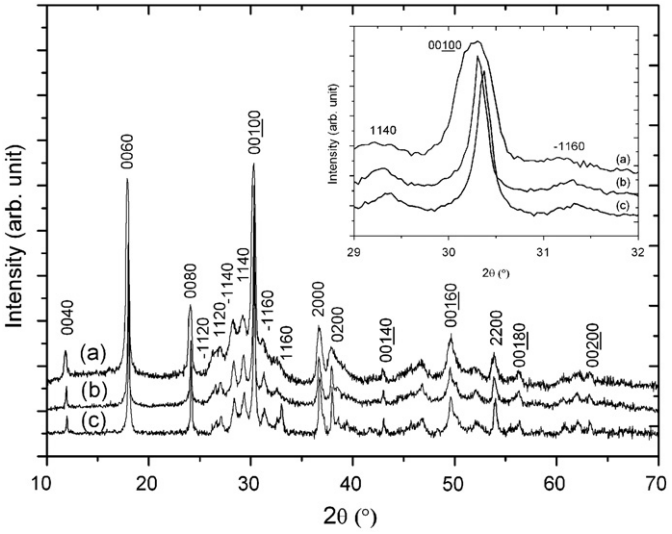

Fig. 1. XRD patterns of BCCO samples prepared by (a) spray-drying, (b) solid state and (c) sol–gel method. Inset: detail between 29 and 32°.

conclusion, the reactions in solution seem very interesting because they lead to more homogeneous samples.

For spray-drying and solid state methods, the valence state of the cobalt (Table 1) was equivalent to the values reported by Morita et al. [33] for $[Ca_2CoO_{3-\delta}]^{RS}[CoO_2]_{1.62}$ and $[(Bi/Pb)_{1.74}Sr_2O_{4-\delta}]^{RS}[CoO_2]_{1.82}$ (3.17 and 3.21, respectively). While a value of 3.35 has been obtained for sol-gel method (Table 1). These three values are lower than V(Co)=3.39 expected for $[Bi_{1.68}Ca_2O_4]^{RS}[CoO_2]_{1.69}$ formula, which could be explained by vacancies in the RS block. The valence state of the cobalt and oxygen content is an important parameter to understand the electrical conductivities of cobaltites [34–36]. This aspect will be developed during the thermoelectric characterization of the materials.

The structure is composed of a RS blocks $[Bi_{1.68}Ca_2O_{4-\delta}]$, formed by 4 layers (CaO–BiO–BiO–CaO), and CoO_2 layers. The incommensurate periodicity, $q=b_1/b_2=1.69$, imposes the superspace formalism for the description of this aperiodic structure [37]. The XRD patterns of BCCO have been indexed with $h\,k\,l\,m$ Miller indices (where k and m Miller indices correspond to RS and CoO_2 blocks, respectively) (Fig. 1) [32]. The full pattern matching analysis was performed using the Jana2000 software [38] (Table 1). As already reported, the cell parameters are close to $a=4.90$ Å, $b_1=4.71$ Å, $b_2=2.79$ Å, $c=14.67$ Å and $\beta=93.32^\circ$ (b_1 for the RS block and b_2 for the CoO_2 layer) [32].

Despite careful preparation of the samples for XRD measurements to minimize preferential orientation effects, all patterns show very intense (0 0 l 0) reflections [30], suggesting platelet geometry of the particles. A zoom of the most intense reflection (i.e., the (0 0 $\underline{10}$ 0) reflection) is shown in the inset of Fig. 1. The peak of the spray-drying sample is significantly broader than those of the other samples. Since one of the contributions to peak broadening is related to the grain size [39], a small particle size can be expected for this sample. This observation is a first proof of the impact of the synthesis method on the microstructure.

These first analyses were confirmed by scanning electron microscopy (SEM) (Fig. 2). The samples are all formed by microplates, but their size and particle size distribution change from one sample to another. In agreement with the observations of XRD patterns, the smallest particles (inferior to 5 μm in the *ab* plane) are obtained by the spray-drying technique (Fig. 2b). The classic solid state method (Fig. 2c) leads to larger particles (inferior to 10 μm in the *ab* plane) while the sol–gel sample (Fig. 2d) is made up of aggregates with typical size between 10 and 20 μm.

In addition to small particle size, a narrow particle size distribution is observed for the sample prepared by spray-drying

Table 1
Cation ratios, valence state of the cobalt and crystallographic parameters of BCCO samples.

Sample	Analyzed Composition Bi: Ca: Co	V(Co)	a (Å)	b_1 (Å)	b_2 (Å)	c (Å)	β (°)	$q = b_1/b_2$
BCCO powder [30]	1.7: 2: 2	–	4.9069(4)	4.7135(7)	2.7878(9)	14.668(5)	93.32(1)	1.6907(2)
BCCO single crystal [32]	1.69: 2: 1.68	–						
Spray drying technique	1.67: 2: 1.71	3.15	4.89(6)	4.72(2)	2.78(7)	14.70(2)	93.5(9)	1.69(4)
Solid State reaction	1.69: 2: 1.93	3.13	4.89(1)	4.72(5)	2.78(10)	14.68(9)	93.3(5)	1.69(4)
Sol Gel method	1.69: 2: 1.67	3.35	4.89(6)	4.70(9)	2.78(3)	14.66(6)	93.4(3)	1.69(1)

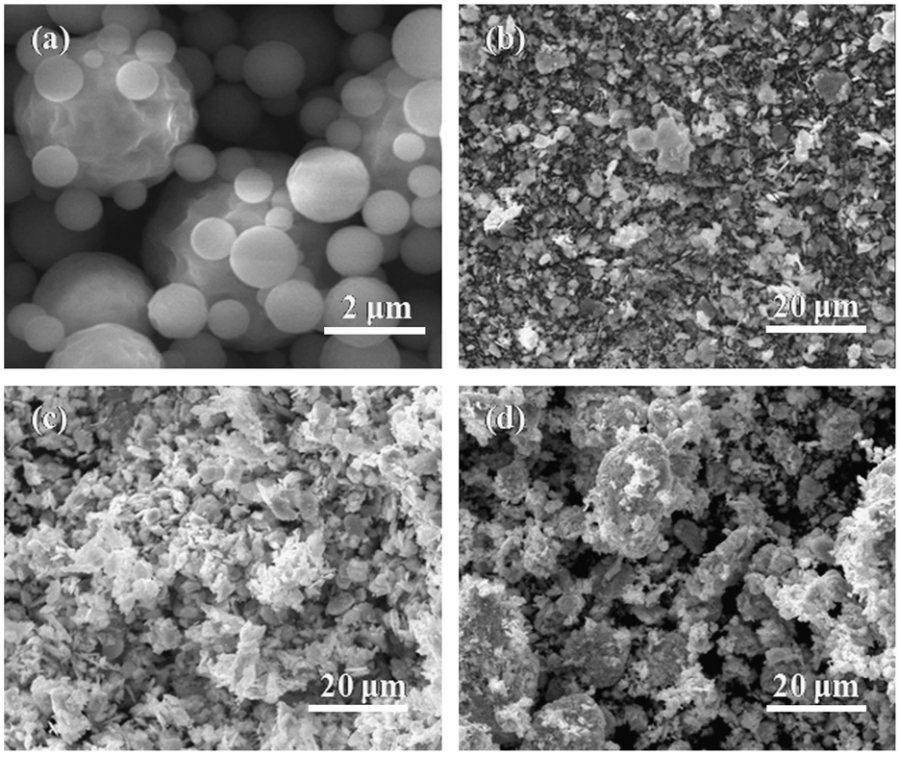

Fig. 2. SEM images of (a) BCCO spray-dried precursor and BCCO samples prepared by (b) spray-drying, (c) solid state and (d) sol–gel method.

technique (Fig. 2a and b). This feature is an asset of this method and probably results from the fact that the precursor after spray-drying is formed of spherical particles inferior to 3 μm with a good particle size distribution (Fig. 2a). Van Driessche et al. and Motohashi et al. have previously reported similar results for (Bi,Pb)-2223 superconductors [40] and $[(Bi,Pb)_2Ba_2O_{4-\delta}]^{RS}[CoO_2]_2$ thermoelectric oxides [41]. In conclusion, the spray-drying technique results in powders with satisfactory characteristics in terms of stoichiometry, small particle size and narrow size distribution.

3.2. Thermoelectric characteristics

In the figure of merit *ZT*, the electrical conductivity is the parameter most affected by the microstructure of bulk samples. In fact, the different microstructural aspects (such as the grain boundary, the grain size and bulk density) have a great influence on this factor. As already mentioned in the introduction, the grain texturing significantly affects the electrical conductivity of these layered oxides. Consequently, we have decided to study the influence of the packing method on the microstructure and we have packed the powders uniaxially or isostatically. The isostatic pressing, which has not been reported yet in this kind of materials, is considered here for different reasons:

- Higher pressing values can be reached (up to 225 MPa).
- A different orientation distribution of the particles can be observed.

Fig. 3a and b correspond to electron micrographs of cross-sections of spray-drying samples respectively uniaxially and isostatically pressed. As expected for anisotropic particles, the isostatic packing induces a random orientation of the plate-like particle, while uniaxial pressing results in a more parallel stacking. Similar results were observed for the solid state samples. On the contrary, the coexistence of small particles and aggregates in the sol–gel samples appears to lead to randomly oriented grains for both types of packing.

The relative density of the samples (theoretical X-ray density $\sim 6.35\,g/cm^3$) was measured by Archimedes' method. The solid-state samples present the highest density: 88% (uniaxial) and 85% (isostatic). For the spray-drying, the densities of the uniaxial and isostatic samples are smaller than the solid state samples (75% and 65%, respectively). These results are in good agreement with the values reported for conventional method (solid state reaction ~65%) [21]. For the sol–gel samples, the density values are the smallest (uniaxial 52% and isostatic 66%). In this case, the coexistence of small particles and agglomerates has limited the densification of the material.

Fig. 4 shows the temperature dependence of the electrical conductivity (σ) of BCCO samples. For all samples, the conductivity decreases with temperature, which is characteristic of a metallic-like behavior. But differences exist depending on the synthesis method and packing treatment. The electric conductivity of the isostatic spray-drying sample is equivalent to the one of the uniaxial solid state ($\sim 22\,S\,cm^{-1}$ at 325 K). These values are in agreement with the literature [29,30]. The highest electrical conductivities are obtained for the uniaxial spray-drying and isostatic solid state: $\sigma = 56.2$ and $36.22\,S\,cm^{-1}$ at 325 K, respectively. It is surprising that the smallest particles (5 μm for spray-drying sample in the *ab* plane) reach the highest electrical conductivity value ($\sigma = 56.2\,S\,cm^{-1}$ at 325 K) which opposes to the effect of grain boundaries on the transport properties.

The narrow particle size distribution and more homogeneous grain orientation could explain this behavior. Indeed firstly, the homogeneous small grains allow a better connectivity between grains and more homogeneous grain boundaries, which lead to an improvement of the electrical conductivity. Secondly, the uniaxial packing of homogenous platelets induces a better orientation (0 0 l) along the pressed plane (Fig. 3) [42,43]. This feature favors the electrical conduction along the ab plane (CoO_2 layers with low resistivity values) and decreases the one along the c axis

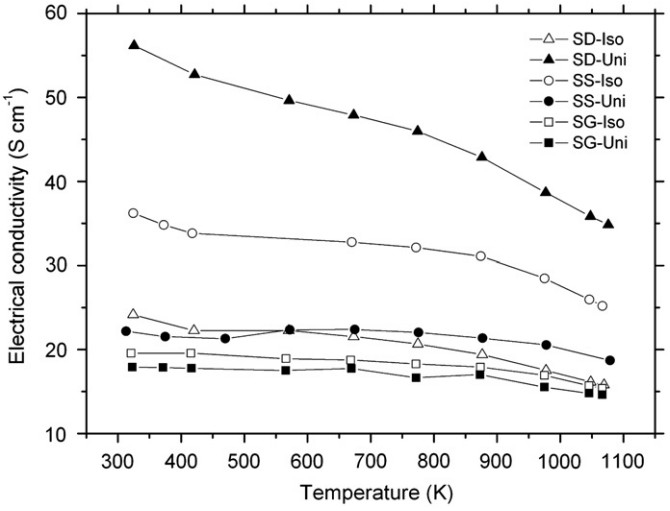

Fig. 4. Electrical conductivity as a function of temperature for BCCO samples. SD = spray-drying, SS = solid state, SG = sol–gel; open and close symbols are the isostatic and uniaxial samples, respectively.

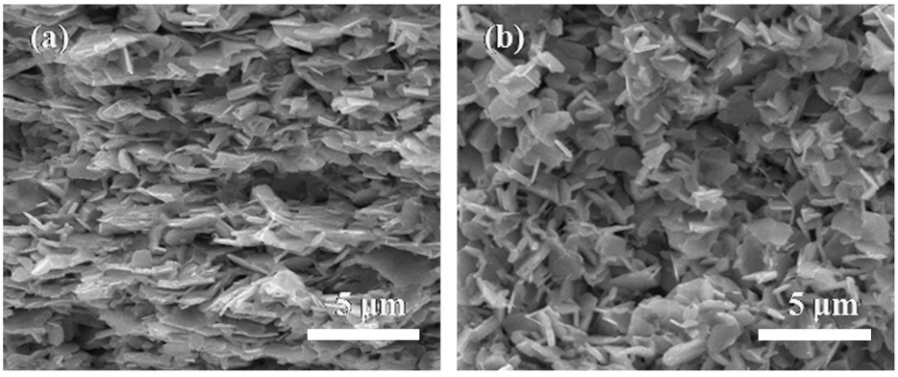

Fig. 3. SEM images of a cross-section of (a) uniaxial (parallel to the pressure direction) and (b) isostatic spray-drying samples.

(through rock-salt layers with high resistivity values). Instead of orientation by high temperature and pressure as in hot-forging, the spray-drying method, by reduction of the particle size distribution, acts like a "chimie douce orientation method". This behavior proves the importance of the particle size distribution to improve the TE properties of these materials although this criterion is rarely considered in the studies of cobaltites. It is interesting to note that the electrical conductivity is even higher than the one reported for the hot-forging method (38.5 S cm^{-1} at 300 K) [30].

For the solid state samples the electrical conductivity of the isostatic sample is higher than the uniaxial sample. The explanation should directly be linked to the larger particle size of the sample (above 10 μm) and not to the grain orientation (Fig. 3). For the isostatic packing, the decrease of the grain boundary number seems mainly to govern the electrical conductivity. For the sol–gel sample, the electrical conductivity values for the different packing methods are almost similar (~19 S cm^{-1} at 325 K). The coexistence of small particles (inferior to 5 μm) with agglomerates (10–20 μm) reduces the orientation effect and the samples density (uniaxial 52% and isostatic 66%).

Finally we compare the cobalt valence in function of the electrical conductivity (Table 1). In general, the electrical conductivity increases with the carrier concentration. In our case, the sample with higher carrier concentration is the sol-gel sample (V(Co)=3.35), which presents the lower electrical conductivity (Fig. 4). Consequently in our samples, the microstructure seems to have a more important impact on the electrical conductivity than the cobalt valence state.

Fig. 5 presents the Seebeck coefficient as a function of temperature. For all samples, positives values are observed indicating a hole carrier conduction (p-type), typical of the layered cobaltites [29,30,43]. The Seebeck coefficient is not significantly affected by the sample preparation. At 325 K, a value of 140 μV K^{-1} is reached and increases almost linearly up to a maximum of 210 μV K^{-1} at 1075 K. These results are in good agreement with those reported in the literature [29]. In conclusion, the Seebeck coefficient, as a bulk property, is less sensitive to interface/surface characteristics.

In Fig. 6, the thermoelectric performance as a function of temperature is evaluated by the power factor ($P=S^2\sigma$). Above 400 K, it increases monotonically with the temperature. Since the behavior of the Seebeck coefficient is similar for the different samples, the power factor is mainly influenced by the evolution of the electrical conductivity. Thus the two highest P values are reached by the samples with the two highest σ values: 0.70 and 1.11 μW K^{-2} cm^{-1} at 325 K for the isostatic solid state and uniaxial spray-drying samples, respectively. The maximum value is obtained for the uniaxial spray-drying sample at ~1050 K, 1.59 μW K^{-2} cm^{-1}. This result is almost twice higher than the one of the uniaxial solid state sample and comparable to the value obtained by hot-forging method [43]. The spray-drying technique seems an interesting method to improve the electric conductivity of these materials. Indeed not hot-forging methods are needed to obtain high electrical conductivity and this method can be used as an industrial scale. These advantages are very interesting for the reduction of the manufacturing cost of these materials.

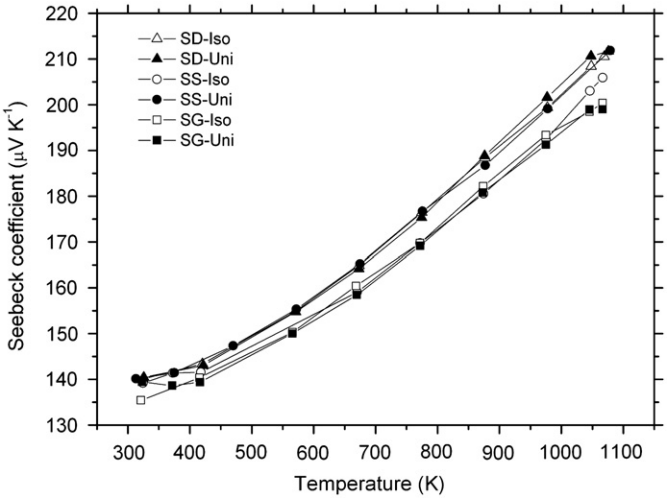

Fig. 5. Seebeck coefficient as a function of temperature for BCCO samples. SD=spray-drying, SS=solid state, SG=sol–gel; open and close symbols are the isostatic and uniaxial samples, respectively.

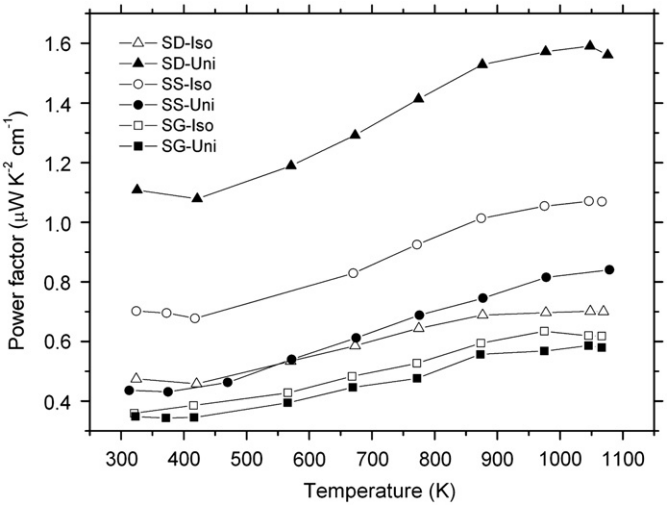

Fig. 6. Power factor as a function of temperature for BCCO samples. SD=spray-drying, SS=solid state, SG=sol–gel; open and close symbols are the isostatic and uniaxial samples, respectively.

4. Conclusion

Single phase $[Bi_{1.68}Ca_2O_{4-\delta}]^{RS}[CoO_2]_{1.69}$ cobaltite has been synthesized by chimie douce methods. The spray-drying technique leads to a reduction of the particles size and size distribution, whereas the sol–gel samples show the coexistence of small particles with agglomerates. The influence of the packing method has also been investigated. The packing treatment or the synthesis method only modified the electrical conductivity of the BCCO materials, indeed the Seebeck coefficient remains almost the same. The highest value of electrical conductivity is obtained for uniaxial spray-drying and isostatic solid state samples. The first case can be explained by a positive reinforcement of the grain orientation by a narrower particle size distribution. For the second one, the random packing of relative large particles seems to increase the electrical conduction. The power factor of the uniaxial spray-drying method is boosted up two times compared with the conventional preparation method. As a conclusion, the spray-drying technique together with uniaxial packing seems to be an interesting method for the cobaltite synthesis from a commercial viewpoint. Indeed this method is less restrictive and presents a lower energetic balance of the synthesis process than the hot-forging technique, although giving equivalent thermoelectric performances. Extensions to other thermoelectric oxides are certainly to be considered.

Acknowledgments

Part of this work was supported by the Belgian Science Policy under the Technology Attraction Pole Program (CHEMAT TAP2/03). H. Muguerra would like to thank the University of Liège for a postdoctoral fellowship.

References

[1] I. Terasaki, Y. Sasago, K. Uchinokura, Phys. Rev. B 56 (1997) R12685.
[2] S. Li, R. Funahashi, I. Matsubara, K. Ueno, H. Yamada, J. Mater. Chem. 9 (1999) 1659.
[3] A.C. Masset, C. Michel, A. Maignan, M. Hervieu, O. Toulemonde, F. Studer B. Raveau, J. Hejtmanek, Phys. Rev. B 62 (2000) 166.
[4] M. Shikano, R. Funahashi, Appl. Phys. Lett. 82 (2003) 1851.
[5] R. Funahashi, I. Matsubara, S. Sodeoka, Appl. Phys. Lett. 76 (2000) 2385.
[6] H. Leligny, D. Grebille, O. Pérez, A.C. Masset, M. Hervieu, C. Michel, B. Raveau, Acta. Cryst. B 56 (1999) 173.
[7] S. Lambert, H. Leligny, D. Grebille, J. Solid State Chem. 160 (2001) 322.
[8] Y. Miyazaki, T. Miura, M. Onoda, M. Uchida, Y. Ishii, Y. Ono, Y. Morii T. Kajitani, Jpn. J. Appl. Phys. 42 (2003) 7467.
[9] M. Hervieu, A. Maignan, C. Michel, V. Hardy, N. Créon, B. Raveau, Phys. Rev. B 67 (2003) 045112.
[10] S. Horii, I. Matsubara, M. Sano, K. Fujie, M. Suzuki, R. Funahashi, M. Shikano, W. Shin, N. Murayama, J.-I. Shimoyama, K. Kishio, Jpn. J. Appl. Phys. 42 (2004) 7018.
[11] D. Pelloquin, S. Hébert, A. Maignan, B. Raveau, Solid State Sci. 6 (2004) 167.
[12] M. Shizuya, M. Isobe, Y. Baba, T. Nagai, Y. Matsui, E. Takayama-Muromachi, J. Solid State Chem. 179 (2006) 3974.
[13] H. Yamauchi, K. Sakai, T. Nagai, Y. Matsui, M. Karppinen, Chem. Mater. 18 (2006) 155.
[14] S. Ishiwata, I. Terasaki, Y. Kusano, M. Takano, J. Phys. Soc. Jpn. 75 (2006) 104716.
[15] M. Shizuya, M. Isobe, Y. Baba, T. Nagai, M. Osada, K. Kosuda, S. Takenouchi Y. Matsui, E. Takayama-Muromachi, J. Solid State Chem. 180 (2007) 249.
[16] S. Li, R. Funahashi, I. Matsubara, K. Ueno, S. Sodeoka, H. Yamada, Chem. Mater. 12 (2000) 2424.
[17] G. Xu, R. Funahashi, M. Shikano, I. Matsubara, Y. Zhou, Appl. Phys. Lett. 80 (2002) 3760.
[18] D. Wang, L. Chen, Q. Wang, J. Li, J. Alloys Compd. 376 (2004) 58.
[19] Q. Yao, D.L. Wang, L.D. Chen, X. Shi, M. Zhou, J. Appl. Phys. 97 (2005) 103905.
[20] M. Prevel, S. Lemonnier, Y. Klein, S. Hébert, D. Chateigner, B. Ouladdiaf, J.G. Noudem, J. Appl. Phys. 98 (2005) 093706.
[21] I. Matsubara, R. Funahashi, T. Takeuchi, S. Sodeoka, J. Appl. Phys. 90 (2001) 462.
[22] Y. Masuda, D. Nagahama, H. Itahara, T. Tani, W.S. Seo, K. Koumoto, J. Mater. Chem. 13 (2003) 1094.
[23] Y. Zhou, I. Matsubara, S. Horii, T. Takeuchi, R. Funahashi, M. Shikano, J. Shimoyama, K. Kishio, W. Shin, N. Izu, N. Murayama, J. Appl. Phys. 93 (2003) 2653.
[24] P.H. Xiang, Y. Kinemuchi, H. Kaga, K. Watari, J. Alloys Compd. 454 (2008) 364.
[25] Y. Song, C.W. Wen, J. Sol–Gel Sci. Technol. 44 (2007) 139.
[26] S. Katsuyama, Y. Takiguchi, M. Ito, J. Mater. Sci. 43 (2008) 3553.
[27] Y.F. Zhang, J.X. Zhang, Q.M. Lu, Q.Y. Zhang, Mater. Lett. 60 (2006) 2443.
[28] Y. Zhang, J. Zhang, Q. Lu, J. Alloys Compd. 399 (2005) 64.
[29] A. Maignan, S. Hébert, M. Hervieu, C. Michel, D. Pelloquin, D. Khomskii, J. Phys.: Condens. Matter 15 (2003) 2711.
[30] E. Guilmeau, M. Pollet, D. Grebille, D. Chateigner, B. Vertruyen, R. Cloots R. Funahashi, B. Ouladiaff, Mater. Res. Bull. 43 (2008) 394.
[31] M. Karppinen, M. Matvejeff, K. Salomäki, H. Yamauchi, J. Mater. Chem. 12 (2002) 1761.
[32] H. Muguerra, D. Grebille, E. Guilmeau, R. Cloots, Inorg. Chem. 47 (2008) 2464.
[33] Y. Morita, J. Poulsen, K. Sakai, T. Motohashi, T. Fujii, I. Terasaki, H. Yamauchi, M. Karppinen, J. Solid State Chem. 177 (2004) 3149.
[34] J.I. Shimoyama, S. Horii, K. Otzschi, M. Sano, K. Kishio, Jpn. J. Appl. Phys. 42 (2003) L194.
[35] C.J. Liu, L.C. Huang, J.S. Wang, Appl. Phys. Lett. 89 (2006) 204102.
[36] J.L. Chen, Y.S. Liu, C.J. Liu, L.C. Huang, C.L. Dong, S.S. Chen, C.L. Chang, J. Phys. D: Appl. Phys. 42 (2009) 135418.
[37] T. Janssen, A. Janner, A. Looijenga, P.M. de Wolff, International Tables for Crystallography, Kluwer Academic Publishers: Dordrecht Vol. C, (1992) 797.
[38] V. Petricek, M. Dusek, L. Palatinus, Jana2000: Crystallographic Computing System (Institute of Physics, Prague, 2000).
[39] A.L. Patterson, Phys. Rev. 56 (1939) 978.
[40] I. Van Driessche, R. Mouton, S. Hoste, Mater. Res. Bull. 31 (1996) 979.
[41] T. Motohashi, Y. Nonaka, K. Sakai, M. Karppinen, H. Yamauchi, J. Appl. Phys. 103 (2008) 033705.
[42] T. Tani, H. Itahara, C. Xia, J. Sugiyama, J. Mater. Chem. 13 (2003) 1865.
[43] E. Guilmeau, M. Mikami, R. Funahashi, J. Mater. Res. 20 (2005) 1002.